Adsorption of dyestuff from aqueous solutions through oxalic acid-modified swede rape straw: Adsorption process and disposal methodology of depleted bioadsorbents

Yanfang Feng [a,b], Dionysios D. Dionysiou [d], Yonghong Wu [b,c], Hui Zhou [c], Lihong Xue [a], Shiying He [a], Linzhang Yang [a,c,*]

[a] Jiangsu Academy of Agriculture Sciences, Nanjing 210014, PR China
[b] State Key Laboratory of Soil and Sustainable Agriculture, Nanjing 210008, PR China
[c] Institute of Soil Science, Chinese Academy of Sciences, Nanjing 210008, PR China
[d] Environmental Engineering and Science Program, University of Cincinnati, Cincinnati, OH 45221-0071, USA

HIGHLIGHTS

- Synthesis of an oxalic acid-modified swede rape straw (SRSOA).
- SRSOA is a competitive and promising substitute for activated carbons.
- SRSOA was systematically characterized and applied to dye adsorption study.
- The disposal methodology of the depleted bioadsorbents was investigated.
- Production of a biochar based on the dye-loaded bioadsorbents for the first time.

GRAPHICAL ABSTRACT
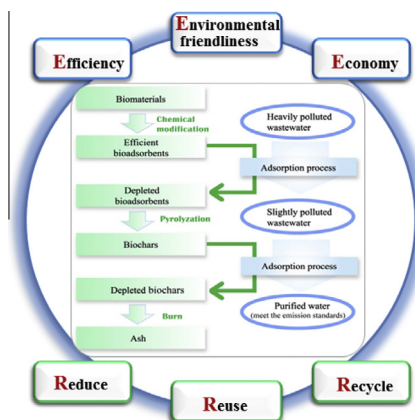
ARTICLE INFO

ABSTRACT

Swede rape straw (*Brassica napus* L.) was modified by oxalic acid under mild conditions producing an efficient dye adsorbent (SRSOA). This low-cost and environmental friendly bioadsorbent was characterized by various techniques and then applied to purify dye-contaminated aqueous solutions. Equilibrium study showed that the Langmuir model demonstrated the best fit to the equilibrium data and the methylene blue (MB) adsorption capacity calculated by this model was 432 mg g^{-1}. The adsorption process and mechanism is also discussed. To properly deal with the dye-loaded bioadsorbents, the disposal methodology is discussed and a biochar based on depleted bioadsorbents was for the first time produced and examined. This method both solved the disposal problem of contaminant-loaded bioadsorbents and produced an useful adsorbent thereafter. The study indicates that SRSOA is a promising substitute for ACs in purifying dye-contaminated wastewater and that producing biochars from contaminant-loaded bioadsorbents maybe a feasible disposal method.

© 2013 Elsevier Ltd. All rights reserved.

1. Introduction

Synthetic dyes need to be treated properly because these contaminants in waters may have carcinogenic, teratogenic and

Nomenclature

A	the constant of Temkin model ($L\,g^{-1}$)	$q_{e,cal}$	the amount of dye adsorbed onto the adsorbents calculated by model at equilibrium ($mg\,g^{-1}$)
b	the constant of Temkin model		
C_0	initial MB concentration ($mg\,L^{-1}$)	q_t	the amount of dye adsorbed onto the adsorbents at time t ($mg\,g^{-1}$)
ΔG^0	Gibbs free energy change ($kJ\,mol^{-1}$)		
ΔH^0	enthalpy change ($kJ\,mol^{-1}$)	q_m	the maximum adsorption capacity for adsorbent ($mg\,g^{-1}$)
ΔS^0	entropy change ($J\,mol^{-1}K^{-1}$)		
k_1	pseudo-first-order kinetic model rate constant (min^{-1})	$q_{m,cal}$	the maximum adsorption capacity calculated by Langmuir model ($mg\,g^{-1}$)
k_2	pseudo-second-order kinetic model rate constant ($mg\,g^{-1}min^{-1}$)	q_d	the amount of dye desorbed from dye-loaded adsorbents ($mg\,g^{-1}$)
K_F	Freundlich adsorption constant ($mg\,g^{-1}$)	R	ideal gas constant ($8.314\,J\,mol^{-1}\,K^{-1}$)
K_{id}	intraparticle rate constant ($mg\,g^{-1}\,min^{-0.5}$)	R^2	linear regression coefficient
m	mass of adsorbent (g)	t	time (min)
n	Freundlich constant	T	temperature (K)
q_e	the amount of dye adsorbed onto the adsorbents at equilibrium ($mg\,g^{-1}$)	V	the volume of solutions (L)

mutagenic effects on both humans and aquatic life (Feng et al., 2011). About 10–20% of the unused dyestuffs, estimated $(0.7–2.0) \times 10^5$ tons annually, are released into water bodies (Dawood and Sen, 2012). Therefore, the treatment of these dye-contaminated effluents with cost-effective and efficient technologies is of high scientific and public interest (Mitter et al., 2012).

Many technologies that remove synthetic dyes from aqueous solutions, such as adsorption, membrane filtration, coagulation, flocculation, microbiological or enzymatic decomposition, advanced oxidation, reverse osmosis and liquid–liquid extraction (Sen et al., 2011), have been studied in recent years. As one of the most employed methods, adsorption technology is frequently applied because of its low investment, simplicity of design, ease of operation and insensitivity to toxic substances in purifying colored solutions (Asgher and Bhatti, 2012).

Activated carbon (AC) is a prevalent adsorbent, but the price is high for large scale water treatment and regeneration of AC is also difficult (Gupta et al., 2011). Consequently, many researchers turned to so-called low-cost adsorbents, such as bio-based adsorbents, mineral-based adsorbents and certain other types of adsorbents (Mitter et al., 2012). But these adsorbents (especially bioadsorbents) have certain obvious disadvantages: (1) the adsorption capacities of crude bioadsorbents are usually too low to be used as substitutes for ACs; (2) many measures, such as chemical modification using H_2SO_4, HCl, HNO_3, H_2O_2, NaOH and some other complex hazardous organic compounds, were applied to improve the adsorption capacity (Liu et al., 2011a), but these treatments may lead to much more serious side effects during the production; (3) even after various complicated modifications, the adsorption capacities of the bioadsorbents were not sufficient; and (4) the prices of these bioadsorbents after various modifications may not be competitive enough (Feng et al., 2012; Fernandez et al., 2010).

Accordingly, swede rape straw (SRS), a crude bioadsorbent with high adsorption capacity, was selected as the precursor and an inexpensive and environmental-friendly chemical, viz., oxalic acid (OA), was applied under mild processing conditions to esterify SRS. Thereafter, an efficient and low-cost bioadsorbent, i.e., swede rape straw modified by oxalic acid (SRSOA), was produced.

To the best of our knowledge, no previous study has investigated the disposal method of contaminant-loaded bioadsorbents, except some conventional desorption studies for bioadsorbents (Mahmoodi et al., 2011). Considering the principle mechanism of adsorption is to transfer the contaminants from aqueous solutions to solid surface, and the contaminants usually do not disappear or degrade, if the contaminant-loaded bioadsorbents are not disposed

of carefully, it may cause some secondary pollution effects, such as contamination of underground water or surface water through a natural desorption process. Consequently, if the low-cost bioadsorbents are to be used in large scale, more attention should be paid to contaminant-loaded bioadsorbents, and disposal methods meeting the "3R" (reduce, reuse and recycle) should be investigated. Desorption is usually unnecessary for such low-cost bioadsorbents because it usually causes serious side-effects to the environment and is not economical. For example, to achieve a sufficiently high desorption rate, these desorption studies usually apply some corrosive acidic or alkaline media during the procedure (Dawood and Sen, 2012; Velghe et al., 2012). The present study, for the first time, proposes a disposal method based on production of biochar from these contaminant-loaded bioadsorbents.

In summary, the main objectives of this study were to (i) produce and characterize the oxalic acid-modified swede rape straw (SRSOA) through material analysis techniques, (ii) describe the adsorption process and adsorption mechanism of MB onto SRSOA, and (iii) present a feasible disposal method for these contaminant-loaded bioadsorbents.

2. Methods

2.1. Adsorbent

The crude swede rape straw was collected in Suzhou Academy of Agriculture Sciences, PR China. The crude bioadsorbent (SRS) was produced according to our previous reported method (Feng et al., 2012). The oxalic acid-modified SRS (i.e., SRSOA) was produced based on a similar procedure reported by Chen (Chen et al., 2003), but with a modification. SRS (20 g) was added to 200 ml of 1.0 M OA, and the mixture was kept in an oven for 2 h at 70 °C. The solid phase was collected through centrifuging and dried at 70 °C for 16 h. The dried biomaterial was then crushed and esterified at 120 °C for 3 h, washed repeatedly with 0.05 M $NaHCO_3$ and successively deionized water. Finally, it was dried overnight at 70 °C, crushed and stored in a brown reagent bottle for subsequent experiments.

The biochar based on the depleted bioadsorbent (i.e., MB loaded bioadsorbent) was produced by the following procedure. The dye-loaded bioadsorbent (SRSOA-MB) was placed in ceramic crucibles, each with a fitting lid, and pyrolyzed in a muffle furnace (Xu et al., 2011). The pyrolysis temperature was raised to 450 °C at a rate of 20 °C min^{-1} and held constant for 4 h, then cooled to room temper-

ature. At last, the biochar was sieved (pore, 250 μm) and stored in an air-tight reagent bottle for further use.

2.2. Chemicals and analytical methods

Methylene blue was purchased from Sinopharm Chemical Reagent Co., Ltd (Shanghai, China). All other chemicals used were of analytical grade. The pH of the solutions was adjusted to 8.0 if not mentioned otherwise.

The MB concentration was measured using a UV–vis spectrophotometer (Shimadzu, UV2450, Japan). All measurements were reproducible within 10% (±SD, $n = 3$). Detailed information on the determination of MB is presented in S.I. 1 (i.e., Supporting Information 1: adsorption process).
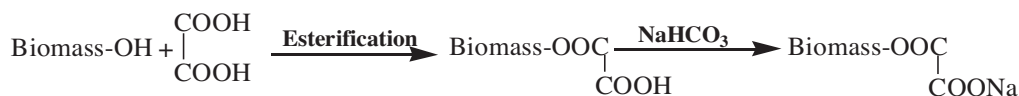
2.3. Adsorption experiment and related theory

The detailed information of adsorption/desorption experiments and relevant mathematic models (isotherm models, kinetic models, etc.) are presented in S.I. 1 and S.I. 2, respectively.

The synthesized bioadsorbents were characterized by Scanning Electron Microscopy (SEM, Quanta 200, FEI, Netherlands) at the magnification of 500×, 1600× and 2600×; Fourier Transform Infrared Spectroscopy (FTIR, Nicolet 360, Thermo Electron Co., USA) at a spectral range of 4000 cm^{-1} to 400 cm^{-1}; particle size distribution analyzing (Mastersizer 2000, Malvern Instruments, UK) and Thermo Gravimetric Analysis (TGA, Pyris 1 TGA, PerkinElmer, USA). Energy Dispersive Spectroscopy (EDS, X2act, INCA, UK) of SRSOA was conducted together with the SEM study. Detailed information on the adsorbent characterization is presented in S.I. 3.

3. Results and discussion

3.1. Characterization of bioadsorbents

3.1.1. SEM-EDS study

SEM (Fig. 1S) was employed to observe the surface morphology of SRS (Fig. 1S-a) and MB-loaded SRSOA (SRSOA-MB, Fig. 1S-b). Crude SRS possessed a rough surface with regular tunnel-like structure, which was due to the remains of cell wall of swede rape straw. Additionally, many small pores on the surface of the tunnel-like structure were observed. The average pore diameter of the small pores (Fig. 1S-a) was 1.09 ± 0.13 μm ($n = 21$, Digimizer). After OA modification, the tunnel-like structure, to a certain degree, was damaged because of the crushing procedure during the modification, but the small pores did not change. After adsorption of MB, the surface morphology of SRSOA changed considerably: the small penetrable pores mentioned above were covered and merely left some faint outline of the pores (inserted figure of Fig. 1S-a and -b). This might be due to the attached dye molecules on the surface of bioadsorbent.

In addition, EDS scanning of SRSOA showed the presence of carbon, oxygen, sulfur, silicon, calcium, chlorine (see Table 1S in S.I. 3). The largest percentages of carbon and oxygen are due to the polysaccharides such as cellulose, hemi cellulose and lignin. The functional groups such as carboxyl group on these polysaccharides may

affect the dye adsorption through changing the surface charge of and surface morphology of bioadsorbent (Feng et al., 2012), and it was confirmed by the following FTIR study.

3.1.2. FTIR analysis

The FTIR spectra (Fig. 2S in S.I. 3) of the three relevant biomaterials (i.e., SRS, SRSOA and SRSOA-MB) are presented to identify the functional groups and the role they played during the adsorption/modification procedure (Liu et al., 2011b).

The most prominent peak change between SRS and SRSOA occurred at around 1747 cm^{-1}, this peak of SRSOA became much sharper than that of SRS which may because a large amount of carboxyl groups (–COO$^-$) appeared after OA modification. Based on this hypothesis, the OA modification process could be expressed as:

$$\text{Biomass-OH} + \overset{\text{COOH}}{\underset{\text{COOH}}{|}} \xrightarrow{\textbf{Esterification}} \text{Biomass-OOC} \overset{}{\underset{\text{COOH}}{|}} \xrightarrow{\textbf{NaHCO}_3} \text{Biomass-OOC} \overset{}{\underset{\text{COONa}}{|}}$$

When comparing the FTIR spectra of SRSOA and SRSOA-MB, it can be found that, after adsorption, new peaks emerged (at around 881 cm^{-1} and 1394 cm^{-1}), peaks heights changed (1740 cm^{-1}) and peaks shifted (1056 cm^{-1}, 2924 cm^{-1}). The possible reasons for the peak changes are listed in Table 2S. Additionally, the newly emerged peaks of SRSOA-MB also indicated that plenty of MB molecules were attached on the surface of SRSOA after the adsorption procedure.

3.2. Operational conditions and environmental effects on adsorption

3.2.1. Particle size distribution and its effects on adsorption

The particle size of SRSOA was somewhat smaller than that of SRS (Fig. 3S-a in S.I. 3). However, lower particle size does not always lead to higher adsorption capacity. The adsorption capacity of bioadsorbents usually reaches a plateau when the particle size decrease to a certain value and the improvement of dye adsorption capacity is limited through decreasing the particle size of bioadsorbents (Asgher and Bhatti, 2012; Gupta et al., 2010). Fig. 3S-b indicates that the q_e value of SRS increased only by 5.97% when the particle size decreased from 0.1–0.15 mm to <0.1 mm. This demonstrates that the dramatic increase in dye-adsorption capacity of SRSOA was not due to the mild decrease of particle size.

3.2.2. Effects of OA concentrations on dye adsorption capacity

Since the change in particle size of bioadsorbents under the present conditions was not the dominant factor that led to the increase of dye-adsorption capacity, OA concentration during the production of bioadsorbents was examined thereafter. The adsorption capacity of SRSOA increased with the increase in OA concentration (Fig. 1a). Higher OA concentrations led to more electronegative oxygen-containing functional groups (such as –COO$^-$) on the surface of SRSOA, which improved the adsorption capacity for the cationic dye. This study demonstrated that the increase of MB adsorption capacity was dominated by OA modification.

3.2.3. Effects of initial dye concentration and contact time on adsorption

Under different initial dye concentrations (300, 500, 700 mg L^{-1}), it is clear that firstly, the q_t values (the amount of MB loaded on
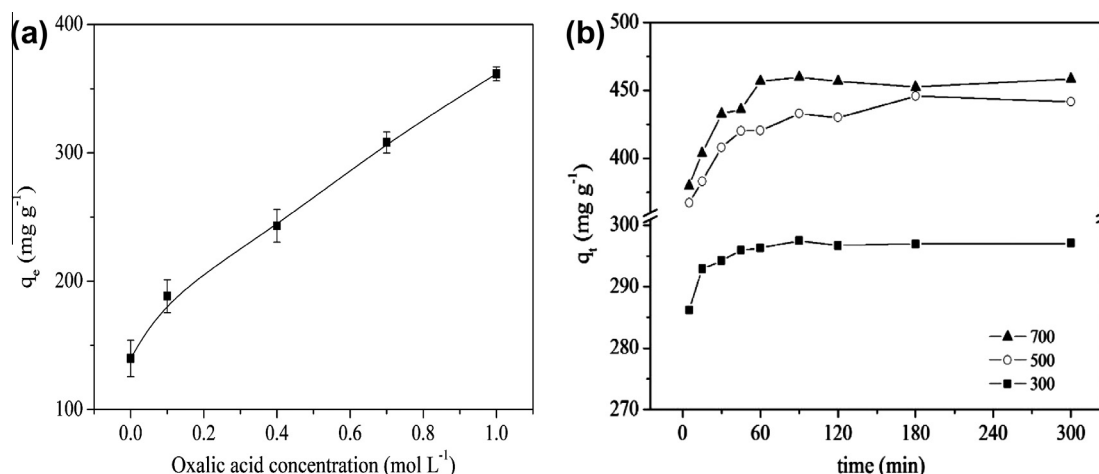
Fig. 1. (a) The effect of oxalic acid concentrations on the amount of MB adsorbed onto SRSOA (experimental conditions: dose = 1 g L^{-1}, initial dye concentration = 500 mg L^{-1}, pH = 8.0). (b) The effect of initial dye concentration and contact time on the adsorption of MB by SRSOA (experimental conditions: dose = 1 g L^{-1}, initial dye concentration = 300, 500, 700 mg L^{-1}, pH = 8.0).

Table 1
Equilibrium parameters for Langmuir, Freundlich and Temkin model, respectively.

Adsorbents	Langmuir			Freundlich			Temkin		
	$q_{m,cal}$ (mg g^{-1})	K_L (L mg^{-1})	R^2	n	K_F (mg g^{-1})	R^2	b	A (L g^{-1})	R^2
SRSOA (25 °C)	432	0.42	0.9999	4.99	166	0.7744	49.0	35.4	0.8887
SRSOA (5 °C)	393	0.44	0.9997	5.29	156	0.7663	55.1	41.3	0.8759
SRS (25 °C)	143	0.05	0.9954	5.43	49	0.9583	125.9	3.6	0.9715

SRSOA at time t) increased with contact time until equilibrium was achieved within 60–180 min. Secondly, the q_t values were higher at greater initial MB concentrations, while the removal percentage was lower. Thirdly, the time needed to achieve equilibrium was longer at higher C_0. These were consistent with our previous studies (Feng et al., 2012).

Dye concentration provides an important driving force to overcome the mass transfer resistance between the solid phase (bioadsorbent) and the liquid phase (water). With the increase of C_0, the driving force increased, which consequently lead to a higher q_t values. But at higher initial concentrations, based on a constant SRSOA dose, the ratio of MB molecule number versus available adsorption site number became higher. As a result, fewer MB molecules (appearing as a lower removal percentage) were adsorbed (Dawood and Sen, 2012).

Additionally, at higher initial concentration, the MB molecules have to penetrate the boundary layer after the rapid attachment on the outer surface of bioadsorbent; while at lower initial MB concentration, the adsorption mainly occurred rapidly on the outer surface of bioadsorbents. Consequently, more time was needed to attain equilibrium for higher initial dye concentrations.

3.3. Adsorption procedure and mechanisms

3.3.1. Equilibrium study
Langmuir model fits best to the experimental isotherm data (Table 1), which means the adsorption of MB onto SRSOA/SRS occurred as a monolayer adsorption and the adsorption affinity on the surface of the bioadsorbents is homogenous in terms of surface functional groups and bonding energy, and the surface contains a finite number of identical adsorption sites (Dawood and Sen, 2012). Further, the calculated MB adsorption capacity ($q_{m,cal}$) of SRSOA was three times higher than that of crude SRS (from 143 mg g^{-1} of SRS to 432 mg g^{-1} of SRSOA, see Table 1). Table 2

summarizes the comparative data of SRSOA with other adsorbents, including some ACs. SRSOA produced under the present conditions is very competitive due to its high adsorption capacity for cationic dyes and may be a feasible substitute for ACs in purifying dye-contaminated wastewater.

3.3.2. Kinetic study
Two widely used kinetic models, i.e., pseudo-first-order and Ho's pseudo-second-order kinetic model, were applied. The parameters for the two kinetic models are shown in Table 3. Table 3 shows the regression coefficients (R^2) of pseudo-second-order kinetic model ($R^2 > 0.999$) at all three initial dye concentrations were higher than those of pseudo-first-order kinetic model. The good fit of the experimental data to the pseudo-second-order kinetic model implies that the rate-limiting step is a chemical sorption between the adsorbate and adsorbent, which is similar to what has been reported in some previous studies (Feng et al., 2011; Mahmoud et al., 2012; Velghe et al., 2012). Additionally, the $q_{e,cal}$ values increased with the increase of initial dye concentrations while the rate constants of pseudo-second-order kinetic model (k_2 values) decreased with the increasing C_0 (Table 3). This could be attributed to the higher competition for the surface sorption sites at higher concentrations (Nethaji and Sivasamy, 2011).

3.3.3. Desorption study
To unveil the mechanism of the adsorption process, a strong acid (HCl), a weak acid (acetic acid), a salt (NaCl) and deionized water were used in a desorption study. Fig. 7S in S.I. 6 demonstrates hydrochloric acid solution is the most efficient chemical in desorbing MB from SRS and SRSOA. Desorption percentages for SRS and SRSOA by HCl solution were 68.8% and 12.4%, respectively. It is known that if the dye molecule (MB) adsorbed onto the adsorbent can be desorbed by deionized water, the adsorption is dominated by weak bonds; if the dye can be desorbed by acid,

Table 2
The comparison of various adsorbents investigated recently by means of MB adsorption capacity.

Adsorbents	MB adsorption capacity (mg g^{-1})	Equilibrium isotherm model	Time needed to achieve equilibrium (h)	Sources
Crude bioadsorbents				
SRS	143	Langmuir	~2	Present study
Poplar leaf	136	Langmuir	3	Han et al. (2012)
Pine cone biomass	110	Langmuir	3	Sen et al. (2011)
Peanut husk	72	Langmuir	3	Song et al. (2011))
Macauba palm	26	Sips	~2	Vieira et al. (2012)
Activated carbon				
AC produced by H$_2$SO$_4$ pretreatment and KOH activation	520	Langmuir	~0.5	Wu et al. (2011)
Filtrasorb 400 (commercial GAC)	319	Langmuir	~0.5	Raposo et al. (2009)
Norit (commercial GAC)	280	Langmuir	~0.5	Raposo et al. (2009)
Picacarb (commercial GAC)	260	Langmuir	~0.5	Raposo et al. (2009)
H$_3$PO$_4$ activated carbon from biomass	145 (mean)	–	–	Girgis et al. (2011)
Chemical modified bioadsorbents				
SRSOA	432	Langmuir	~1	Present study
Wheat straw modified by carboxymethylation	275	Langmuir	3	Zhang et al. (2011)
NaOH-modified rejected tea	242	Langmuir	–	Nasuha and Hameed (2011)
Kapok fiber treated by sodium chlorite	105	–	1	Liu et al. (2012)
HCl treated kenaf fiber char	18	Langmuir	8	Mahmoud et al. (2012)

Table 3
The parameters of pseudo-second-order kinetic model and pseudo-first-order kinetic model at three initial dye concentrations.

C_0 (mg L^{-1})	Pseudo-second-order kinetic model			Pseudo-first-order kinetic model	
	$q_{e,cal}$ (mg g^{-1})	k_2 ($\times 10^{-2}$) (g mg^{-1} min^{-1})	R^2	k_1 ($\times 10^{-3}$) (min^{-1})	R^2
300	298	1.68	0.9999	4.35	0.8851
500	446	0.09	0.9998	3.37	0.8302
700	460	0.15	0.9999	3.19	0.3435

the adsorption is dominated by ion exchange (Chen et al., 2011). The above results imply that ion exchange was an important mechanism in adsorbing MB onto SRS and SRSOA. The low desorption rate for SRSOA may be attributed to the low acid concentration (0.01 M) and high dye adsorption capacity of SRSOA (Velghe et al., 2012).

3.3.4. Thermodynamic study

The thermodynamic parameters are given in Table 4S in S.I. 7. The positive values of ΔH^0 indicate that the adsorption procedure under the present conditions was endothermic. Consequently, the adsorption capacity increases with temperature, and the equilibrium study confirms it (see $q_{e,cal}$ values in Table 1). The negative Gibbs free energy values reveal the spontaneity of the process. Additionally, the variation of energy for physical adsorption is usually substantially smaller than that of chemisorption because physical adsorption is non-specific, on the contrary, chemical adsorption is similar to ordinary chemical reactions in that it is highly specific (Crini and Badot, 2008). The dividing line between physical adsorption and chemical adsorption is not very sharp. Usually, if the values of ΔH^0 are lower than 40 kJ mol^{-1}, and the values of ΔG^0 are within the ranges of −20 and 0 kJ mol^{-1}, physical adsorption is the dominant mechanism (Feng et al., 2011; Mahmoodi et al., 2010). According to Table 4S in S.I. 7, both ΔH^0 values and ΔG^0 values meet the above criteria, which demonstrates that the adsorption of MB by SRSOA is dominated by physical adsorption.

3.3.5. Adsorption mechanism

For a solid–liquid adsorption system, the solute transfer is usually characterized by boundary layer diffusion, intraparticle diffusion or both, and the controlling step of the adsorption could be intraparticle and/or external diffusion procedure (Dawood and Sen, 2012). The adsorption of MB onto SRSOA may first be controlled by external diffusion and then by intraparticle diffusion. In order to better understand the adsorption mechanism, the kinetic data are typically analyzed by the intraparticle diffusion model (Eq. 13 in S.I. 2).

The adsorption process can be divided into three steps (Fig. 6S-a). The first step completed within several minutes is dominated by external mass transfer, which is probably due to a strong electrostatic attraction between adsorbate (MB) and external surface of adsorbent (SRSOA). The second step complete within about 1 h, is the rate limiting step, and it may be attributed to the intraparticle diffusion of MB molecules through the pores of SRSOA. The third step is the equilibrium stage because the low adsorbate concentrations in the solutions make the intraparticle diffusion of MB molecules slow (Feng et al., 2011; Mittal et al., 2012). In the second stage, the C values (Eq. 13) increased when the initial MB concentration increased from 300 mg g^{-1} to 700 mg g^{-1} (Table 3S in S.I. 5), it indicates the increase of the boundary layer thickness. Meanwhile, the K_{id} values increased with C_0, too, since the increase in MB concentration leads to increase in adsorption driving force, which consequently causes an enhanced MB diffusion rate (Weng et al., 2009). Further, the regression curves for all three initial dye concentrations of stage two, if extended, did not pass through the origin. This implies that intraparticle diffusion is not the only mechanism that dominates the rate-limiting process (Özcan et al., 2005).

The boundary layer effect may control the rate of mass transfer in the slow-adsorption step, which is corroborated by the analysis of dynamic data from Boyd's model (Eq. 14 in S.I. 2). The plots (Fig. 6S-b) are linear only at the initial period and do not pass through the origin, it means in this period the rate-limiting mechanism is external mass transfer and then intraparticle diffusion (Tang et al., 2012). At high MB initial concentrations, the figures
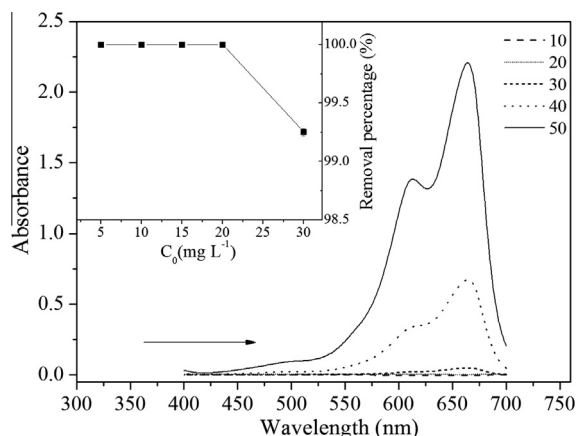
Fig. 2. The removal percentage and the UV–vis spectra of the solutions after adsorption by SRSOA-MB based biochar (conditions: initial MB concentrations = 5, 10, 15, 20, 30, 40, 50 mg L^{-1}; adsorbent: biochar produced by MB-loaded SRSOA; adsorbent dosage = 1 g L^{-1}; the UV–vis spectra were based on non-diluted waste water).
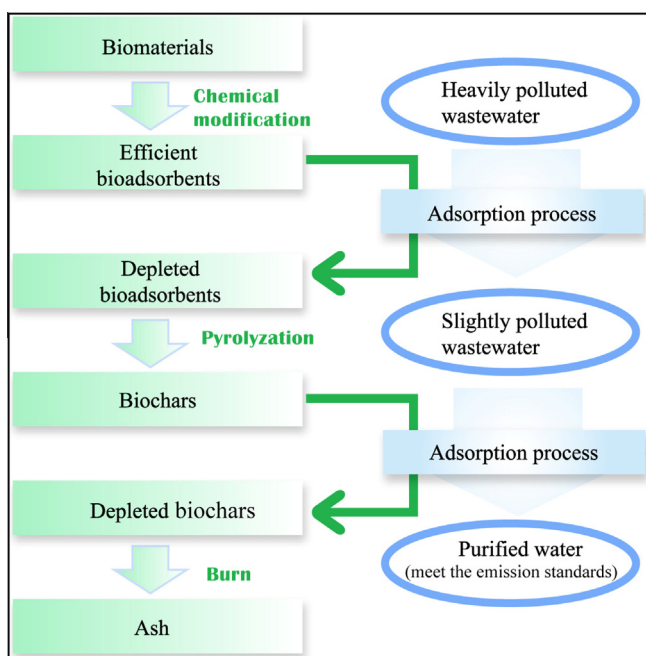

Fig. 3. A circulation system for bioadsorbent recycle & wastewater purification.

obtained do not exhibit linearity, which confirms the involvement of film diffusion mechanism at higher concentrations (Mittal et al., 2012).

3.4. Biochar derived from depleted (dye-loaded) bioadsorbents

To properly deal with the dye-loaded bioadsorbents, a biochar was produced from the depleted biomaterial. This biochar was used to purify the low-concentration artificial wastewater (Fig. 2). The results showed the adsorption capacity for MB was significantly lower than that of SRSOA, most probably because some of the functional groups (such as –COO$^-$ and phenolic –OH) (Xu et al., 2011) on the surface of SRSOA were destroyed by the pyrolysis and the pore structures of biochars were not well developed under the present conditions. However, at lower initial MB concentrations, the removal percentage for this biochar was significantly

higher than that of common bioadsorbents. The MB concentrations were undetectable (i.e., the removal percentages were virtually 100%) given that the initial dye concentrations were lower than 30 mg g^{-1} in the present experiment (Fig. 2). This means that the biochar based on SRSOA-MB adsorbent can resolve two issues simultaneously: (1) avoiding secondary pollution caused by SRSOA-MB, and (2) purifying low concentration dye wastewater. Moreover, biochars are also biofuel (Xu et al., 2011). Thus, a circulation system for bioadsorbent recycles and wastewater purification has been established (see Fig. 3). According to this protocol, the depleted bioadsorbents can be reduced (through pyrolysis), reused (purifying low-concentration of dye contaminated wastewater), recycled and properly disposed of (completely decompose to ash); meanwhile, wastewater can be purified.

3.5. Economical evaluation

The cost of adsorbents is one of the key factors that we must consider if they are to be applied to actual use in wastewater purification. The cost of SRSOA is dramatically affected by the oxalic acid consumed. If oxalic acid is efficiently used, to produce 1 kg SRSOA, the OA consumed would be about 0.47 kg. The corresponding price of consumed OA would be approximately 100 USD for producing one metric ton of SRSOA (according to the largest B2B online trading market in China). Compared with commercial activated carbon, the price of which is about 500–2500 USD per metric ton (Chen et al., 2011; Ferrero, 2010), the cost for SRSOA may be an economically competitive substitute in purifying dye-contaminated wastewater.

4. Conclusions

This study indicates that oxalic acid-modified swede rape straw can be used as an efficient, economical, environmentally-friendly and easily-produced bioadsorbent for purifying dye-contaminated wastewater. According to the Langmuir model, the maximum monolayer adsorption capacity for MB was 432 mg g^{-1}. Moreover, this study, for the first time, investigated the disposal method for contaminant-loaded bioadsorbents. A biochar derived from contaminant-loaded bioadsorbents was produced through pyrolysis and reused for adsorption. Consequently, the contaminant-loaded bioadsorbent can be reduced, reused, recycled and properly disposed of; meanwhile, the wastewater can be purified. The disposal method was promising and more studies are warranted in further studies.

Acknowledgements

Appendix A. Supplementary data

Supplementary data (detailed information about (1) adsorption process; (2) theory and related equations; (3) characteristics of relevant adsorbents (such as SEM, EDS scanning, FTIR spectra, particle size analysis and TGA study); (4) effects of adsorbent dose on adsorption; (5) plots and parameters for intraparticle diffusion model and Boyd's model; (6) desorption study and (7) thermodynamic

study) associated with this article can be found, in the online version, at http://dx.doi.org/10.1016/j.biortech.2013.03.146.

References

Asgher, M., Bhatti, H.N., 2012. Evaluation of thermodynamics and effect of chemical treatments on sorption potential of Citrus waste biomass for removal of anionic dyes from aqueous solutions. Ecol. Eng. 38 (1), 79–85.

Chen, J.P., Wu, S., Chong, K.-H., 2003. Surface modification of a granular activated carbon by citric acid for enhancement of copper adsorption. Carbon 41 (10), 1979–1986.

Chen, H., Zhao, J., Wu, J., Dai, G., 2011. Isotherm, thermodynamic, kinetics and adsorption mechanism studies of methyl orange by surfactant modified silkworm exuviae. J. Hazard. Mater. 192 (1), 246–254.

Crini, G., Badot, P.-M., 2008. Application of chitosan, a natural aminopolysaccharide, for dye removal from aqueous solutions by adsorption processes using batch studies: a review of recent literature. Prog. Polym. Sci. 33 (4), 399–447.

Dawood, S., Sen, T.K., 2012. Removal of anionic dye Congo red from aqueous solution by raw pine and acid-treated pine cone powder as adsorbent: equilibrium, thermodynamic, kinetics, mechanism and process design. Water Res. 46 (6), 1933–1946.

Feng, Y., Yang, F., Wang, Y., Ma, L., Wu, Y., Kerr, P.G., Yang, L., 2011. Basic dye adsorption onto an agro-based waste material – Sesame hull (Sesamum indicum L.). Bioresour. Technol. 102 (22), 10280–10285.

Feng, Y., Zhou, H., Liu, G., Qiao, J., Wang, J., Lu, H., Yang, L., Wu, Y., 2012. Methylene blue adsorption onto swede rape straw (Brassica napus L.) modified by tartaric acid: equilibrium, kinetic and adsorption mechanisms. Bioresour. Technol. 125, 138–144.

Fernandez, M.E., Nunell, G.V., Bonelli, P.R., Cukierman, A.L., 2010. Effectiveness of Cupressus sempervirens cones as biosorbent for the removal of basic dyes from aqueous solutions in batch and dynamic modes. Bioresour. Technol. 101 (24), 9500–9507.

Ferrero, F., 2010. Adsorption of Methylene Blue on magnesium silicate: kinetics, equilibria and comparison with other adsorbents. J. Environ. Sci. 22 (3), 467–473.

Girgis, B.S., Soliman, A.M., Fathy, N.A., 2011. Development of micro-mesoporous carbons from several seed hulls under varying conditions of activation. Microporous Mesoporous Mater. 142 (2–3), 518–525.

Gupta, V.K., Jain, R., Siddiqui, M.N., Saleh, T.A., Agarwal, S., Malati, S., Pathak, D., 2010. Equilibrium and thermodynamic studies on the adsorption of the dye Rhodamine-B onto mustard cake and activated carbon. J. Chem. Eng. Data 55 (11), 5225–5229.

Gupta, V.K., Agarwal, S., Saleh, T.A., 2011. Chromium removal by combining the magnetic properties of iron oxide with adsorption properties of carbon nanotubes. Water Res. 45 (6), 2207–2212.

Han, X., Niu, X., Ma, X., 2012. Adsorption characteristics of methylene blue on poplar leaf in batch mode: equilibrium, kinetics and thermodynamics. Korean J. Chem. Eng. 29 (4), 494–502.

Liu, H., Cai, X., Wang, Y., Chen, J., 2011a. Adsorption mechanism-based screening of cyclodextrin polymers for adsorption and separation of pesticides from water. Water Res. 45 (11), 3499–3511.

Liu, H., Yang, F., Zheng, Y., Kang, J., Qu, J., Chen, J.P., 2011b. Improvement of metal adsorption onto chitosan/Sargassum sp. composite sorbent by an innovative ion-imprint technology. Water Res. 45 (1), 145–154.

Liu, Y., Wang, J., Zheng, Y., Wang, A., 2012. Adsorption of methylene blue by kapok fiber treated by sodium chlorite optimized with response surface methodology. Chem. Eng. J. 184, 248–255.

Mahmoodi, N.M., Arami, M., Bahrami, H., Khorramfar, S., 2010. Novel biosorbent (Canola hull): surface characterization and dye removal ability at different cationic dye concentrations. Desalination 264 (1–2), 134–142.

Mahmoodi, N.M., Hayati, B., Arami, M., Lan, C., 2011. Adsorption of textile dyes on Pine Cone from colored wastewater: kinetic, equilibrium and thermodynamic studies. Desalination 268 (1–3), 117–125.

Mahmoud, D.K., Salleh, M.A.M., Karim, W.A.W.A., Idris, A., Abidin, Z.Z., 2012. Batch adsorption of basic dye using acid treated kenaf fibre char: equilibrium, kinetic and thermodynamic studies. Chem. Eng. J. 181–182, 449–457.

Mittal, A., Thakur, V., Gajbe, V., 2012. Evaluation of adsorption characteristics of an anionic azo dye Brilliant Yellow onto hen feathers in aqueous solutions. Environ. Sci. Pollut. Res., 1–10.

Mitter, E., dos Santos, G., de Almeida, É., Morão, L., Rodrigues, H., Corso, C., 2012. Analysis of acid Alizarin Violet N dye removal using sugarcane bagasse as adsorbent. Water Air Soil Pollut. 223 (2), 765–770.

Nasuha, N., Hameed, B.H., 2011. Adsorption of methylene blue from aqueous solution onto NaOH-modified rejected tea. Chem. Eng. J. 166 (2), 783–786.

Nethaji, S., Sivasamy, A., 2011. Adsorptive removal of an acid dye by lignocellulosic waste biomass activated carbon: equilibrium and kinetic studies. Chemosphere 82 (10), 1367–1372.

Özcan, A.S., Erdem, B., Özcan, A., 2005. Adsorption of Acid Blue 193 from aqueous solutions onto BTMA-bentonite. Colloids Surf. A 266 (1–3), 73–81.

Raposo, F., De La Rubia, M.A., Borja, R., 2009. Methylene blue number as useful indicator to evaluate the adsorptive capacity of granular activated carbon in batch mode: influence of adsorbate/adsorbent mass ratio and particle size. J. Hazard. Mater. 165 (1–3), 291–299.

Sen, T., Afroze, S., Ang, H., 2011. Equilibrium, kinetics and mechanism of removal of Methylene Blue from aqueous solution by adsorption onto pine cone biomass of Pinus radiata. Water Air Soil Pollut. 218 (1), 499–515.

Song, J.Y., Zou, W.H., Bian, Y.Y., Su, F.Y., Han, R.P., 2011. Adsorption characteristics of methylene blue by peanut husk in batch and column modes. Desalination 265 (1–3), 119–125.

Tang, H., Zhou, W., Zhang, L., 2012. Adsorption isotherms and kinetics studies of malachite green on chitin hydrogels. J. Hazard. Mater. 209–210, 218–225.

Velghe, I., Carleer, R., Yperman, J., Schreurs, S., D'Haen, J., 2012. Characterisation of adsorbents prepared by pyrolysis of sludge and sludge/disposal filter cake mix. Water Res. 46 (8), 2783–2794.

Vieira, S.S., Magriotis, Z.M., Santos, N.A.V., Cardoso, M.d.G., Saczk, A.A., 2012. Macauba palm (Acrocomia aculeata) cake from biodiesel processing: an efficient and low cost substrate for the adsorption of dyes. Chem. Eng. J. 183, 152–161.

Weng, C.-H., Lin, Y.-T., Tzeng, T.-W., 2009. Removal of methylene blue from aqueous solution by adsorption onto pineapple leaf powder. J. Hazard. Mater. 170 (1), 417–424.

Wu, F.-C., Wu, P.-H., Tseng, R.-L., Juang, R.-S., 2011. Preparation of novel activated carbons from H_2SO_4-pretreated corncob hulls with KOH activation for quick adsorption of dye and 4-chlorophenol. J. Environ. Manage. 92 (3), 708–713.

Xu, R.K., Xiao, S.-C., Yuan, J.-H., Zhao, A.-Z., 2011. Adsorption of methyl violet from aqueous solutions by the biochars derived from crop residues. Bioresour. Technol. 102 (22), 10293–10298.

Zhang, W., Yan, H., Li, H., Jiang, Z., Dong, L., Kan, X., Yang, H., Li, A., Cheng, R., 2011. Removal of dyes from aqueous solutions by straw based adsorbents: batch and column studies. Chem. Eng. J. 168 (3), 1120–1127.